Surface Modification of Mesoporous, Macroporous, and Amorphous Silica with Catalytically Active Polyoxometalate Clusters

Bret J. S. Johnson and Andreas Stein*

Department of Chemistry, University of Minnesota, Minneapolis, Minnesota 55455

Received December 17, 1999

Transition-metal-substituted polyoxometalates (TMSP) of the type $[M^{II}(H_2O)PW_{11}O_{39}]^{5-}$ (M = Co, Zn) and $[SiW_9O_{37}\{Co^{II}(H_2O)\}_3]^{10-}$ have been chemically anchored to modified macroporous (400 nm pores), mesoporous (2.8 nm pores), and amorphous silica surfaces. The materials were characterized by solid-state ^{31}P MAS NMR, UV−vis, FT-IR spectroscopy, and N_2 adsorption experiments to verify cluster attachment and the structure of the TMSP on the support. On the basis of the spectroscopic evidence, clusters were attached datively to the surface, and the integrity of the $[CoPW_{11}]$ cluster was maintained for nonaqueous impregnation with $TBA_5[CoPW_{11}]$; partial degradation of the cluster occurred when it was impregnated from aqueous solution using the $K_5[CoPW_{11}]$ salt. Both the amine surface groups and the cobalt centers in the clusters were found to be necessary to prevent cluster loss during washing or reaction processes. The catalytic activities of the supported TMSP clusters were tested by the epoxidation of cyclohexene to cyclohexene oxide in the presence of isobutyraldehyde. The percent conversion of the substrate and the amount of product formed per unit time were similar for $[CoPW_{11}]$ clusters on each of the three silica supports, but slightly lower than for purely homogeneous reactions. $[SiW_9Co_3]$ clusters with three available cobalt centers exhibited higher catalytic activity with nearly identical performance on a silica support or in homogeneous solution.

Introduction

Keggin-type polyoxometalate (POM) clusters such as $[EM_{12}O_{40}]^{x-}$ (E = Si, $x = 4$; E = P, $x = 3$; M = W, Mo) are an important class of inorganic oxide materials.[1,2] They are discrete metal−oxygen clusters composed of early transition metals in their highest oxidation state. POMs are strong Brønsted acids when the counterion is a proton; they have a high charge and can be reversibly reduced. Some applications of POMs include stains for electron microscopy, acid catalysts, and ion-exchange materials. Important subclasses of POM clusters include lacunary POMs. These are incomplete clusters, which are missing one or more addenda atoms (W, Mo). Unsaturated POMs bind several different species including organosilanes, -germanes, -stannanes,[3−5] and many transition metals.[6] Applications of transition-metal-substituted polyoxometalates (TMSP) include uses as catalysts that take advantage of open coordination sites on the transition metal or its oxidation/reduction potential.

Several recent studies have investigated the role of TMSP clusters in oxidative catalysis.[7−14] Polyoxometalates of this type are considered to be inorganic porphyrins,[15] large inert ligands, which leave accessible coordination sites on the transition metal center. In these ‘inorganic porphyrins’ the lacunary polyoxometalate coordinates the transition metal with five formally O^{2-} ligands, while the last coordination site on the metal is occupied by an aqua ligand. The aqua ligand of most TMSPs can be displaced in aqueous media by ligands such as pyridines or ammonia.[16,17] In nonaqueous media, the transition metal site can be dehydrated and is then quite reactive toward other ligands.[18] The W atoms are in their highest oxidation state and are therefore oxidatively resistant unlike organic porphyrins, which tend to oxidize and degrade after a few catalytic cycles. Oxidative catalytic reactions take place by oxidation of the transition metal site and are typical surface-type catalytic processes in which the reaction rate is directly proportional to the surface area of the catalyst.[19] Most current uses of TMSPs are in homogeneous catalysis,[7−12,14] making separation of the catalyst an added step in the reaction process.

The goal of this research was to prepare a heterogeneous catalyst that incorporated the properties of both the polyoxometalate (acid catalysis, oxidation catalysis, ion-exchange) and a high surface area silica support. Silica supports can be tailored by various templating techniques to give different surface areas and pore size distributions, affecting transport of reagents to the catalytic sites and catalyst selectivity. This paper describes a method of modifying amine-functionalized porous silica

---

(1) Pope, M. T. *Heteropoly and Isopolyoxometalates*; Springer-Verlag: New York, 1983.
(2) *Chem. Rev.* **1998**, *98*, special issue on polyoxometalates.
(3) Knoth, W. H. *J. Am. Chem. Soc.* **1979**, *101*, 759.
(4) Judeinstein, P.; Deprun, C.; Nadjo, L. *J. Chem. Soc., Dalton Trans.* **1991**, 1991.
(5) Ammari, N.; Hervé, G.; Thouvenot, R. *New J. Chem.* **1991**, *15*, 607.
(6) Weakley, T. J. R.; Malik, S. A. *J. Inorg. Nucl. Chem.* **1967**, *29*, 2935.
(7) Neumann, R.; Abu-Gnim, C. *J. Chem. Soc., Chem. Commun.* **1989**, 1324.
(8) Neumann, R.; Abu-Gnim, C. *J. Am. Chem. Soc.* **1990**, *112*, 6025.
(9) Mizuno, N.; Tateishi, M.; Hirose, T.; Iwamoto, M. *Chem. Lett.* **1993**, 1985.
(10) Mizuno, N.; Hirose, T.; Tateishi, M.; Iwamoto, M. *Chem. Lett.* **1993**, 1839.
(11) Neumann, R.; Dahan, M. *J. Chem. Soc., Chem. Commun.* **1995**, 171.
(12) Kholdeeva, O. A.; Grigoriev, V. A.; Maksimov, G. M.; Fedotov, M. A.; Golovin, A. V.; Zamaraev, K. I. *J. Mol. Catal. A* **1996**, *114*, 123.
(13) Khenkin, A. M.; Rosenberger, A.; Neumann, R. *J. Catal.* **1999**, *182*, 82.
(14) Indira, V.; Joy, P. A.; Gopinathan, S.; Gopinathan, C. *Indian J. Chem.* **1998**, *37A*, 473.
(15) Khenkin, A. M.; Hill, C. L. *J. Am. Chem. Soc.* **1993**, *115*, 8178.
(16) Woo, H. Y.; So, H.; Pope, M. T. *J. Am. Chem. Soc.* **1996**, *118*, 621.
(17) Baker, L. C. W.; Figgis, J. S. *J. Am. Chem. Soc.* **1970**, *92*, 3794.
(18) Katsoulis, D. E.; Pope, M. T. *J. Am. Chem. Soc.* **1984**, *106*, 2737.
(19) Okuhara, T.; Mizuno, N.; Misono, M. *Adv. Catal.* **1996**, *41*, 113.

10.1021/ic991440y CCC: $20.00

supports with transition-metal-substituted polyoxometalates. The open coordination site available to these TMSP clusters allows them to be chemically anchored to the surfaces of the functionalized supports. Supporting TMSP clusters on high surface area porous solids may allow fine dispersion of the TMSP over the entire surface with greater access to the active sites of well-separated TMSP clusters.

Three different silica supports were used in this study: amorphous fumed silica, mesoporous silica (MCM-41) with a pore size of 2.8 nm (synthesized by a surfactant templating process),[20] and macroporous silica consisting of a 3-dimensional array of 400 nm pores surrounded by amorphous silica walls approximately 65 nm thick (synthesized by a latex sphere templating technique).[21,22] The silica walls in the macroporous solid contained themselves a wide distribution of mesopores. Three TMSP clusters were used, two monosubstituted POMs, $[M(H_2O)PW_{11}O_{39}]^{5-}$ ($[MPW_{11}]$, M = Co^{II} or Zn^{II}) and one trisubstituted POM, $[SiW_9O_{37}\{Co(H_2O)\}_3]^{10-}$ ($[SiW_9Co_3]$). Previous studies of polyoxometalates supported on amorphous silica and MCM-41 surfaces had focused on the free acids of Keggin-type POMs introduced onto the silica by incipient wetness.[23−29] For these materials it was possible that the polyoxometalate could be removed from the surface by washing. In other recent papers, the silica surface was first functionalized with an amine ligand and treated with free-acids of POM clusters.[30−32] When protonated, the amines held the POMs to the surface by electrostatic interactions. In the present study, the silica surface was also functionalized with an amine ligand. However, because the impregnated POM was not a free-acid but a transition-metal-substituted POM, the transition metal site was bound by the surface amines and anchored to the surface through dative bonding. The result was to minimize leaching of the cluster by washing or during a reaction cycle.

Experimental Section

Materials. Amorphous silica (Cab-osil M-5), Fluka Chemical; tetraethyl orthosilicate (TEOS), cetyltrimethylammonium bromide, tetrabutylammonium bromide, Aliquat 336, sodium metasilicate, cobalt acetate tetrahydrate, zinc acetate dihydrate, and potassium bicarbonate, Aldrich; sodium tungstate dihydrate, Mallinckrodt; sodium phosphate dibasic, Fisher Scientific Co.; 3-aminopropyltriethoxy silane, Gelest, Inc.

Preparations of $K_5[\alpha\text{-}Co^{II}(H_2O)PW_{11}O_{39}]$, $K_5[\alpha\text{-}Zn(H_2O)PW_{11}O_{39}]$, $Na_{10}[\beta\text{-}SiW_9O_{34}]$, $K_7[\alpha\text{-}PW_{11}O_{39}]$, and $K_{10-x}H_x[\beta\text{-}SiW_9O_{37}\{Co^{II}(H_2O)\}_3]$ were adapted from literature methods.[33−35]

$K_5[\alpha\text{-}Co^{II}(H_2O)PW_{11}O_{39}]$. FT-IR of the potassium salt: 1077, 1057, 960, 888, 817, 752, 715, 512 cm^{-1}. DR-UV−vis: 494 sh, 518 sh, 562 nm. The FT-IR and UV−vis spectra are in agreement with spectra obtained from the literature.[33,36] Tetrabutylammonium salts were prepared by metathesis. EA for $K_5[Co(H_2O)PW_{11}O_{39}]\cdot 66H_2O$ (wt % found/calculated): W (48.84/48.88%), Co (1.64/1.42%), P (0.789/0.749%).

$K_5[\alpha\text{-}Zn^{II}(H_2O)PW_{11}O_{39:}]$. FT-IR of the potassium salt: 1092, 1053, 957, 888, 828, 758, 709, 509 cm^{-1}. Tetrabutylammonium salts were prepared by metathesis. The FT-IR spectrum is in agreement with published literature.[33,36] ^{31}P NMR: −11.7 ppm. EA for $K_5[Zn(H_2O)PW_{11}O_{39}]\cdot 25H_2O$ (wt % found/calculated): W (59.24/59.37%), Zn (2.206/1.920%), P (1.010/0.9093%)

$K_7[\alpha\text{-}PW_{11}O_{39}]$. FT-IR: 1091, 1043, 951, 903, 854, 808, 732, 592, 509 cm^{-1}, in agreement with the literature.[36] EA for $K_7[\alpha\text{-}PW_{11}O_{39}]\cdot 16H_2O$ (wt % found/calculated): W (62.21/62.43), P (1.079/0.956), K (9.227/8.450).

$Na_{10}[\beta\text{-}SiW_9O_{34}]\cdot xH_2O$. FT-IR: 988, 922, 867, 816, 745, 712, 551, 528 cm^{-1}, in agreement with literature.[34] EA for $Na_{10}[\beta\text{-}SiW_9O_{34}]\cdot 30H_2O$ (wt % found/calculated): W (55.18/55.22%), Si (1.039/0.937%), Na (7.71/7.67%).

$K_{10-x}H_x[\beta\text{-}SiW_9O_{37}\{Co^{II}(H_2O)\}_3]\cdot xH_2O$. FT-IR of $K_{10-x}H_x[SiW_9O_{37}\{Co^{II}(H_2O)\}_3]$: 987, 944, 891, 798, 719, 536 cm^{-1}. DR-UV−vis: 486, 516, 548 nm. FT-IR and UV−vis spectra are consistent with the literature.[35] Tetrabutylammonium salts were prepared by metathesis. EA for $K_9H[SiW_9O_{37}\{Co(H_2O)\}_3]\cdot 51H_2O$ (wt % found/calculated): W (43.77/43.79%), Co (4.237/4.680%), Si (1.522/0.743%), K (9.337/9.313%).

MCM-41. MCM-41 was synthesized following the method of Corma et al.[37] Extraction of the surfactant was performed by dispersing the white solid in 200 mL of MeOH to which 3.78 g of concentrated HCl had been added. This was refluxed for 24 h, filtered, and washed with H_2O and MeOH until the pH was neutral. An FT-IR spectrum of the extracted support confirmed the removal of the surfactant. Powder XRD showed a typical hexagonal MCM-41 pattern with four distinct peaks, $d_{100} = 35.9$ Å, $d_{110} = 21.5$ Å, $d_{200} = 18.8$ Å, $d_{210} = 13.4$ Å.

Macroporous Silica. This was synthesized using a latex sphere templating technique.[22] Centrifuged polystyrene spheres (1.5 g) of 500 nm diameter (± 8%) were packed into a glass tube (i.d. 1 cm) fitted with glass wool at the outlet. N_2 gas was passed over the spheres for 5 min. A 20 mL solution of EtOH and TEOS (50 wt %/wt) containing approximately 0.25 mL of concentrated HCl was then added to the tube. This was forced through the tube with N_2 gas. When a sufficient amount of silicate precursor had passed through the tube (enough to “wet” the spheres, approximately 15 mL), the flow of N_2 was stopped and the mixture was dried. The white composite powder was calcined in air for 10 h at 550 °C to remove the latex spheres. Due to shrinkage during processing, the final voids were ca. 400 nm in diameter.

Grafting Technique. 1.0 g of dried silica support was dispersed in 50 mL of toluene. To this was added 1.5 g of $(EtO)_3SiCH_2CH_2CH_2NH_2$. This mixture was stirred vigorously at room temperature for 1 h and refluxed for 2 h. The silica support was isolated by filtration to obtain a white powder of amine-grafted silica support. EA (wt %) amine-grafted silica: C (4.05), N (1.41), H (0.91). Amine-grafted MCM-41: C (11.97), N (3.93), H (3.07). Amine-grafted macroporous silica: C (3.80), N (1.19), H (0.79). Hydrogen analysis includes surface hydroxyls and occluded H_2O.

Impregnation with TMSP Cluster. Impregnation was performed on modified silica supports with $X_5[MPW_{11}]$ (X = K^+, TBA^+; M = Co, Zn), $K_{10-x}H_x[SiW_9Co_3]$, and $K_7[PW_{11}]$ and on unmodified silica (Cab-osil) with $K_5[CoPW_{11}]$ and $K_7[PW_{11}]$. A typical synthesis was as follows. The support (0.250 g) was dispersed in 25 mL of H_2O at pH

---

(20) Beck, J. S.; Vartuli, J. C.; Roth, W. J.; Leonowicz, M. E.; Kresge, K. T.; Schmitt, K. D.; Chu, W. T.-W.; Olson, D. H.; Sheppard, E. W.; McCullen, S. B.; Higgins, J. B.; Schlenker, J. L. *J. Am. Chem. Soc.* **1992**, *114*, 10834.

(21) Holland, B. T.; Blanford, C. F.; Stein, A. *Science* **1998**, *281*, 538.

(22) Holland, B. T.; Blanford, C. F.; Do, T.; Stein, A. *Chem. Mater.* **1999**, *11*, 795.

(23) Izumi, Y.; Hasebe, R.; Urabe, K. *J. Catal.* **1983**, *84*, 402.

(24) Kresge, C. T.; Marler, D. O.; Rav, G. S.; Rose, B. H. U.S. Patent 5,366,945, 1994.

(25) Chu, W.; Yang, X.; Shan, Y.; Ye, X.; Wu, Y. *Catal. Lett.* **1996**, 201.

(26) Khozhevnikov, I. V.; Kloestra, K. R.; Sinnema, A.; Zandbergen, H. W.; van Bekkum, H. *J. Mol. Catal. A* **1996**, *114*, 287.

(27) Ghanbari-Siahkali, A.; Philippou, A.; Dwyer, J.; Anderson, M. W. *Appl. Catal. A* **2000**, *192*, 57.

(28) Blasco, T.; Corma, A.; Martínez, A.; Martínez-Escolano, P. *J. Catal.* **1998**, *177*, 306.

(29) Marme, F.; Coudurier, G.; Védrine, J. C. *Microporous Mesoporous Mater.* **1998**, *22*, 151.

(30) Khenkin, A. M.; Neumann, R.; Sorokin, A. B.; Tuel, A. *Catal. Lett.* **1999**, *63*, 189.

(31) Kamada, M.; Nishijima, H.; Kera, Y. *Bull. Chem. Soc. Jpn.* **1993**, *66*, 3565−3570.

(32) Kamada, M.; Kominami, H.; Kera, Y. *J. Colloid Interface Sci.* **1996**, *182*, 297.

(33) Weakley, T. J. R. *J. Chem. Soc., Dalton Trans.* **1973**, 341.

(34) Tézé, A.; Hervé, G. *Inorganic Syntheses*; John Wiley & Sons: New York, 1990; Vol. 27, p 89.

(35) Liu, J.; Ortéga, F.; Sethuraman, P.; Katsoulis, D. E.; Costello, C. E.; Pope, M. T. *J. Chem. Soc., Dalton Trans.* **1992**, 1901.

(36) Thouvenot, R.; Rocchioccioli-Deltcheff, C. *J. Chem. Res., Synop.* **1977**, 46.

(37) Corma, A.; Kan, Q.; Navarro, M. T.; Pérez-Pariente, J.; Rey, F. *Chem. Mater.* **1997**, *9*, 2123.

Table 1. Elemental Analysis of TMSP−Silica Materials

	% W	% M[a]	% P	% K	% Si	% C	% N	% H[b]	% TMSP
A: amorphous silica + $K_5[CoPW_{11}]$	0.3239	0.0245	<0.01	0.0959	36.73				0
B: amorphous silica + $K_7[PW_{11}]$	0.0596		<0.01	0.0461	37.03				0
C: amorphous silica + amine + $K_5[CoPW_{11}]$	17.36	0.8699	0.3195	<0.01	26.26				30.7
	16.36	0.6845	0.3012	0.0645	30.52	3.06	1.11	1.07	26.9
D: amorphous silica + amine + $K_7[PW_{11}]$	5.145		0.0829	<0.01	33.29				7.0
E: amorphous silica + $K_5[CoPW_{11}]$, incipient wetness	17.82	0.7745	0.2887	3.2846	23.53				30.5
F: sample (E) after washing	0.0705	0.0210	<0.01	0.0761	35.87				0
G: amorphous silica + amine + $TBA_5[CoPW_{11}]$	8.150	0.2331	0.1363		34.74	8.69	2.63	2.00	16.3
H: amorphous silica + amine + $K_5[ZnPW_{11}]$	15.72	0.6548	0.3166	<0.01	27.32				25.6
I: amorphous silica + amine + $TBA_5[ZnPW_{11}]$	8.544	0.3123	0.1524		30.15	8.95	2.58	1.99	18.4
J: amorphous silica + amine + $K_{10-x}H_x[SiW_9Co_3]$	12.87	1.053		0.0377	29.88	3.07	1.12	1.04	17.4
K: macroporous silica + amine + $K_5[CoPW_{11}]$	10.32	0.4499	0.1827	0.2268	34.57	2.63	0.79	0.79	17.2
L: MCM-41 + amine + $K_5[CoPW_{11}]$	16.46	0.7740	0.3109	<0.01	26.79	8.41	2.90	2.47	28.6
M: MCM-41 + amine + $TBA_5[CoPW_{11}]$	4.836	0.1384	0.0862		30.54	9.01	3.64	2.92	9.9

[a] M = Co^{II} or Zn^{II}. [b] Hydrogen analysis includes surface hydroxyls and occluded H_2O.

6−7. To this was added 0.125 g of the intended TMSP cluster dissolved in a minimal amount of water. The mixture was then stirred for 24 h at room temperature, filtered, and washed with 100 mL of H_2O to obtain the TMSP-impregnated silica support. Impregnation was also carried out in nonaqueous media with the use of tetrabutylammonium salts of the TMSP clusters. The silica support (0.250 g) was dispersed in 25 mL of CH_3CN, and 0.125 g $TBA_5[MPW_{11}]$ (M = Co, Zn) in 1−2 mL of CH_3CN was added. The TMSP−silica material was filtered off and washed with CH_3CN after 24 h. Another sample was prepared by the method of incipient wetness. 0.250 g of unmodified silica was stirred with a solution of 0.125 g of $K_5[CoPW_{11}]$ at 80 °C until the water was evaporated. The sample was then heated at 120 °C for 2 h. After analysis, this sample was washed with 100 mL H_2O. Elemental analysis of TMSP−silica materials is provided in Table 1.

Catalysis. Catalytic tests were performed using the following reaction mixture: 7 mL $CDCl_3$, 0.75 μmol supported TMSP (mass added was calculated from the weight percent of TMSP determined by EA of the TMSP−silica materials), 3000 μmol isobutyraldehyde, 750 μmol cyclohexene, and 224.2 μmol benzene (internal standard). The reactants were mixed in a round-bottom flask fitted with a gas inlet and a reflux condenser. O_2 was passed over the reaction solution at a rate of 10 mL/min while the solution was stirred for 1 h. The reaction was also carried out in air with identical results. At the completion of the reaction, the mixture was filtered on a 0.2 μm filter and the products purged with N_2 gas before being directly sampled by ^1H and ^{13}C NMR. Reaction products were quantified by ^1H NMR. In homogeneous reactions, stoichiometric amounts of $[CH_3N^+(CH_2)_7CH_3)_3]$ (Aliquat 336) were added to the TBA salts of the TMSP clusters to allow dissolution in $CDCl_3$.

Physical Measurements. FT-IR spectra were collected on a Nicolet Magna 760 FT-IR with 2 cm^{-1} resolution. Samples were prepared as KBr pellets for mid-IR (4000−400 cm^{-1}) and polyethylene pellets for far-IR (700−75 cm^{-1}). UV−vis absorption spectra were collected on a Hewlett-Packard 8452A diode array UV−visible spectrophotometer with a Labsphere RSA-HP-84 reflectance spectroscopy accessory. Reflectance data were converted to $f(R_\infty)$ using the Kubelka−Munk equation. N_2 adsorption experiments were performed on a Micrometrics ASAP 2000 sorption analyzer. ^1H and proton-decoupled ^{13}C NMR spectra were collected on a Varian Unity Inova 300 MHz spectrometer operating at 299.957 MHz. Spectra were recorded from samples in $CDCl_3$ in 5 mm (o.d.) tubes and referenced to tetramethylsilane. ^{29}Si and ^{31}P solid-state MAS NMR spectra (single pulse) were collected on a Chemagnetics 400 MHz spectrometer and referenced to tetramethylsilane and 85% H_3PO_4, respectively. Powder XRD was performed on a Siemens D5005 X-ray diffractometer with Cu Kα radiation. Carbon, nitrogen, and hydrogen analyses were performed by Atlantic Microlabs, Norcross, GA. All other elements were determined by the Department of Geology, University of Minnesota, using an inductively coupled plasma source and mass-spectrometry (ICP/MS).

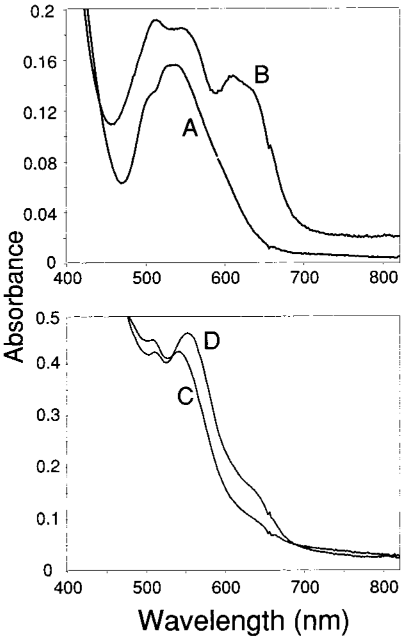

Figure 1. Solution UV−vis spectra. Top: (A) $K_5[CoPW_{11}]$; (B) $K_5[CoPW_{11}]$ + *n*-butylamine. Bottom: (C) $K_9H[SiW_9Co_3]$; (D) $K_9H[SiW_9Co_3]$ + *n*-butylamine. The new absorption peaks between 600 and 640 nm in the top spectra and at 642 nm in the bottom spectra are due to coordination of the amine to the Co^{II} center.

Results and Discussion

Synthesis and Characterization of TMSP Clusters. Transition-metal-substituted polyoxometalates (TMSP) were synthesized using established literature methods.[33−35] The FT-IR spectra in the range 1100−500 cm^{-1} provide characteristic fingerprints for POM clusters and were used for structural confirmation.

To probe the effects of ligand coordination to the TMSP cluster, a solution UV−vis spectroscopy experiment was conducted before analyzing TMSPs supported on amine functionalized supports. Spectral features due to changes in the local Co^{II} environment before and after the introduction of a ligand could then be compared with spectra of the supported TMSP samples. Figure 1 shows the solution UV−vis spectra of both the mono- and tricobalt-substituted TMSP clusters and the changes brought on by the introduction of *n*-butylamine. The main features of Co^{II} substituted POM clusters were an oxygen−tungsten charge-transfer band at 375 nm and a $^4T_{1g}(P) \leftarrow {}^4T_{1g}(F)$ transition typical for octahedral Co^{II} with six oxygen bound ligands at 562 nm, with small shoulders at 518 and 494 nm. The addition of *n*-butylamine to the TMSP solution resulted in the displacement of coordinated water by the organic ligand. This caused a lowering of the symmetry of the Co^{II} site and a subsequent splitting of the $^4T_{1g}(P)$ band[33] into E_g and A_{2g}

Scheme 1

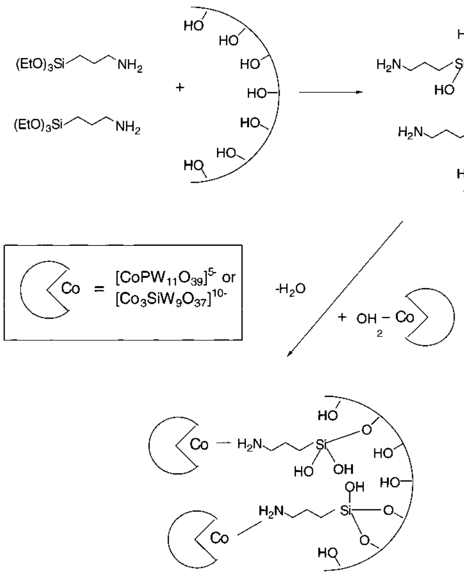

components.[38] As a result, new absorbances were observed between 600 and 640 nm (λ_{max} = 616, 638sh nm) in the spectrum for $K_5[CoPW_{11}]$ and at 642 for $K_9H[SiW_9Co_3]$ (Figure 1B and D).

Supporting TMSP Clusters on Silica Supports. The supported TMSP materials were synthesized by a relatively simple two-step method presented in Scheme 1.

After synthesis and removal of any templates, the silica supports were treated with $(EtO)_3SiCH_2CH_2CH_2NH_2$ in refluxing toluene to attach this ligand to surface silanol groups.[39,40] A solid-state ^{29}Si MAS NMR spectrum of amorphous silica grafted with propylamine groups confirmed the presence of organo-silanes on the surface; in addition to the $(SiO)_3\mathbf{Si}OH$ (Q^3) and $\mathbf{Si}(OSi)_4$ (Q^4) resonances of the support at −102 and −112 ppm, the spectrum showed peaks at −59 and −68 ppm, corresponding to $R\mathbf{Si}(OH)_2OSi$ (T^1) and $R\mathbf{Si}(OH)(OSi)_2$ (T^2), respectively ($R = CH_2CH_2CH_2NH_2$). These indicate that most of the grafted functional groups were bound to the surface with one or two Si−O−Si linkages. The organically modified silica was then stirred in an aqueous solution of $K_5[MPW_{11}]$ (M = Co, Zn) or $K_9H[SiW_9Co_3]$. The synthesis was also performed in nonaqueous media, by employing TBA^+ salts of the TMSP clusters and acetonitrile as the solvent.

The measured amounts of grafted amine ligands and TMSP clusters on different supports are presented in Table 2. The ratio of mmoles of amine per gram of silica was largest on MCM-41 because of the high surface area (see Table 3) and large number of available surface hydroxyl groups after surfactant extraction. In case of the macroporous silica sample, the template was removed by calcination, resulting in a lower number of surface hydroxyls and a smaller number of amine groups grafted to the surface. On the other hand, the average amine surface density was lowest on MCM-41 (1.7 amines/nm^2), compared to 3 amines/nm^2 on amorphous silica and 2.6 amines/nm^2 on macroporous silica. After impregnation with TMSP clusters, only a fraction of the amines was bound to the clusters. Macroporous silica contained one TMSP cluster per 9 amines, and amorphous silica had one TMSP cluster per 8 amines. The fraction of attached clusters in MCM-41 was even lower, with one TMSP cluster per 20 amines, presumably due to partial pore blockage with TMSP clusters. Much of the surface of MCM-41 was confined within the channels and was less accessible than external surfaces or surfaces in larger pore materials (see section on N_2 adsorption).

Table 2. Loading of Propyl Amine and TMSP on Impregnated Silica Supports

TMSP−silica material	mmol amine[a]/g SiO_2	mmol TMSP/g SiO_2	TMSP/ amine
macroporous silica + amine/$K_5[CoPW_{11}]$	0.76	0.084	0.11
MCM-41 + amine/$K_5[CoPW_{11}]$	3.61	0.181	0.05
amorphous silica + amine/$K_5[CoPW_{11}]$	1.21	0.150	0.12
MCM-41 + amine/$TBA_5[CoPW_{11}]$	3.61	0.038	0.05
amorphous silica + amine/$TBA_5[CoPW_{11}]$	1.21	0.055	0.05
amorphous silica + amine/$K_{10}[SiW_9Co_3]$	1.26	0.108	0.08

[a] Moles of amines based on N elemental analysis.

Table 3. Comparison of N_2 Adsorption Results for Macro- and Mesoporous Silica

	BET surface area (m^2/g)[a]	BJH pore volume (mL/g)[a]
macroporous silica	196	0.41
grafted with propylamine	129 (143)	0.26 (0.29)
grafted and impregnated with $K_5[CoPW_{11}]$	76 (96)	0.20 (0.26)
MCM-41	980	0.90
grafted with propylamine	603 (873)	0.38 (0.55)
grafted and impregnated with $K_5[CoPW_{11}]$	473 (861)	0.35 (0.63)

[a] Numbers without parentheses correspond to m^2/g or mL/g of the whole sample. Numbers in parentheses correspond to m^2/g or to mL/g of silica only, excluding organic groups or clusters.

Amine-modified supports impregnated with $[CoPW_{11}]$ clusters using TBA^+ salts in acetonitrile solution contained lower cluster loadings and lower TMSP/amine ratios than samples prepared from K^+ salts in aqueous solution. The lowering of the TMSP loading is most likely due to the formation of TBA-TMSP ion-pairs in solution; such ion-pairs have been noted in solutions of $TBA_4[SiW_{12}]$ at concentration levels similar to those used in our study.[41] The TMSP was therefore much larger and the Co^{II} site more hindered, decreasing the likelihood of binding to a surface ligand.

A series of impregnation experiments were performed to determine the effects of the surface ligand and the transition metal center. Both amine-modified and unmodified amorphous silica, and POM clusters with ($K_5[CoPW_{11}]$) and without ($K_7[PW_{11}]$) cobalt centers, were employed. The experiments indicated that the combination of ligand-modified silica and cobalt-containing POM clusters resulted in the highest cluster retention on washed silica surfaces, see Table 1 samples A−D. Lacunary $[PW_{11}]^{7-}$ was retained to a lesser degree on ligand-modified silica, which may be due to electrostatic interactions between protonated amine ligands and anionic POM clusters. Unmodified silica failed to retain any complete POM clusters, lacunary or TMSP, although trace amounts of W, Co, and P were detected. A sample of unmodified silica was also impregnated with $K_5[CoPW_{11}]$ by the method of incipient wetness (E). In this way, TMSP clusters could be introduced to the silica surface at loadings very similar to those in materials

---

(38) Drago, R. S. *Physical Methods for Chemists*, 2nd ed.; Saunders College/Harcourt Brace Jovanovich: New York, 1992.

(39) De Hann, J. W.; Van Den Bogaert, H. M.; Ponjeé, J. J.; Van De Ven, L. J. M. *J. Coll. Interface Sci.* **1986**, *110*, 519.

(40) Moller, K.; Bein, T. *Chem. Mater.* **1998**, *10*, 2950.

(41) Fournier, M.; Thouvenot, R.; Rocchiccioli-Deitcheff, C. *J. Chem. Soc., Faraday Trans.* **1991**, *87*, 349.

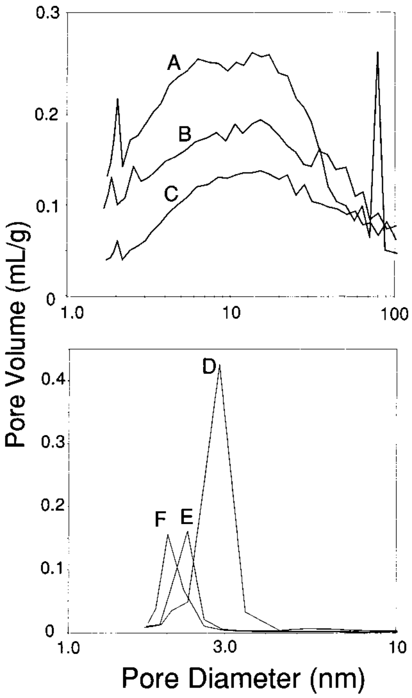

Figure 2. Pore size distribution plots from N_2 adsorption experiments. Top: (A) macroporous silica; (B) macroporous silica grafted with propylamine; (C) macroporous silica−amine + $K_5[CoPW_{11}]$. Bottom: (D) MCM-41, extracted; (E) MCM-41 grafted with propylamine; (F) MCM-41−amine + $K_5[CoPW_{11}]$.

prepared from ligand-modified silica with TMSP clusters. However, when washing this sample, the TMSP cluster was completely removed from the surface (F), as indicated by elemental analysis and DR-UV−vis spectroscopy, where absorptions due to the TMSP were absent.

Nitrogen adsorption studies and BET calculations on the macro- and mesoporous silica supports revealed that the surface areas decreased after grafting of the amine groups and after impregnation with the cluster, see Table 3 and Figure 2. The macroporous silica support consisted of a three-dimensional array of large pores (400 nm) with amorphous silica walls approximately 65 nm thick. Mesopores with a broad distribution of pore diameters around 10.0 nm were present within the walls (Figure 2 top). The surface area was comparable to that of the amorphous silica used in these studies (Cab-osil silica, 200 ± 25 m^2/g). Introduction of organic groups and TMSP clusters reduced both the surface area and the pore volume. The drop in pore volume among the smaller mesopores in the walls of the macroporous supports was most likely due to filling of these pores with TMSP clusters. For the MCM-41 sample, the decrease in pore volume between grafting of the amine and introduction of the TMSP was small (Table 3 and Figure 2 bottom). A reasonable explanation for this observation was that many of the TMSP clusters were not introduced into the pores, consistent with the relatively low cluster density found in this sample. The BJH pore size of the MCM-41 sample was 2.8 nm, and the size of the TMSP was 1.0 nm.[42] Attachment of a TMSP cluster to a propylamine ligand extending into the pore channel (ca. 0.82 nm) would decrease the pore opening to less than half of its original diameter, thus effectively blocking other clusters from entering that channel. This would reduce the surface area accessible to TMSP clusters, but N_2 could still enter the pores. Thus the material retained a large portion of the pore volume.

It has been noted that POM clusters can break down on silica surfaces when the weight loading is very low (below 20 wt %).[43] Several characterization techniques were therefore performed to identify the structure of the TMSP cluster after addition to the supports and also to probe how the TMSP was anchored to the surface. FT-IR spectroscopy was used to determine the presence of the cluster on the silica surfaces. Peak assignments are based on literature values.[4,36] In the mid-IR range, the broad ν_{Si-O} stretching absorption at 1050 cm^{-1} overlapped with some of the cluster peaks. Peaks due to P−O asymmetric stretches (1077, 1057 cm^{-1}) were completely obscured by the presence of silica. Absorptions from terminal W−O bonds appeared at 960 cm^{-1} for $K_5[CoPW_{11}]$. In supported samples a small shoulder on a silica peak at 950 cm^{-1} was observed for all of the TMSP-impregnated supports (see Figure 3). Absorptions for W−O−W stretching modes appeared at 890 cm^{-1} for the unsupported and supported TMSP clusters. In the far-IR region, the strongest absorptions for $K_5[CoPW_{11}]$ were W−O−W bending modes observed at 371 cm^{-1} and a shoulder at 333 cm^{-1} (Figure 3A). These frequencies are intermediate between those observed in the Keggin cluster ($[PW_{12}]$) (382, 338 cm^{-1}), and the $[PW_{11}]$ cluster (360, 330 cm^{-1}),[4,36] as one might expect for the transition-metal-substituted cluster. Another peak appeared at 264 cm^{-1} and was also assigned to the TMSP cluster. All of these spectral features were observed for the TMSP-treated silica supports (Figure 3B, C, and D) but not for the untreated support (Figure 3E), confirming the presence of TMSP cluster on the support.

DR-UV−vis spectroscopy was used for characterization of the Co^{II} site (Figure 4) in the pink Co^{II} TMSP-impregnated supports. The peak shapes and positions of TMSPs in solution and in the solid state were similar (compare Figure 1A and C to Figure 4A and F). Spectra of TMSPs supported on amine-modified silica and solution TMSPs reacted with an amine ligand were also similar. Supported $[CoPW_{11}]$ clusters showed the appearance of a weak absorption around 628 nm when incorporated as K^+ salts (Figure 4B) and a more prominent absorption at 638 nm for the TBA^+ salt (Figure 4C and Figure 5C). The splitting of the $^4T_{1g}(P)$ band was more resolved in the TBA^+ salts, possibly because of a stronger interaction between the surface amine and the Co^{II} site. The trisubstituted $[SiW_9Co_3]$−silica materials produced a distinct new band at 647 nm (Figure 4G). By comparison to the solution UV spectra in the presence of an amine ligand, the new peaks were due to the displacement of the water ligand from the Co^{II} within the TMSP cluster and coordination of the surface amine. Further evidence of coordination between $[CoPW_{11}]$ and surface ligands was found by comparing DR-UV−vis spectra of samples prepared from amine-modified silica and TMSP clusters to those prepared by incipient wetness. Incipient wetness samples did not exhibit a split in the main absorbance peak in the DR-UV−vis spectra and had a spectrum nearly identical to that of an unsupported TMSP cluster (see Figure 5A). Dilution on silica resulted in overall decreased absorbance values from the TMSP clusters.

The cluster structure was also probed by ^{31}P solid-state MAS NMR spectra. Because of the paramagnetic nature of cobalt the diamagnetic zinc derivatives were used as model compounds, which bind to the surface in the same manner as cobalt-substituted clusters. The ^{31}P resonance for $TBA_5[ZnPW_{11}]$ was at −11.7 ppm, consistent with the literature value (Figure 6A).[44]

---

(42) Fuchs, J.; Thiele, A.; Palm, R. *Z. Naturforsch.* **1980**, *36b*, 161.

(43) Sinnema, A.; Jansen, R. J. J.; Pamin, K.; van Bekkum, H. *Catal. Lett.* **1995**, *30*, 241.

(44) Jorris, T. L.; Kozik, M.; Casan-Pastor, N.; Domaille, P. J.; Finke, R. G.; Miller, W. K.; Baker, L. C. W. *J. Am. Chem. Soc.* **1987**, *109*, 7402.

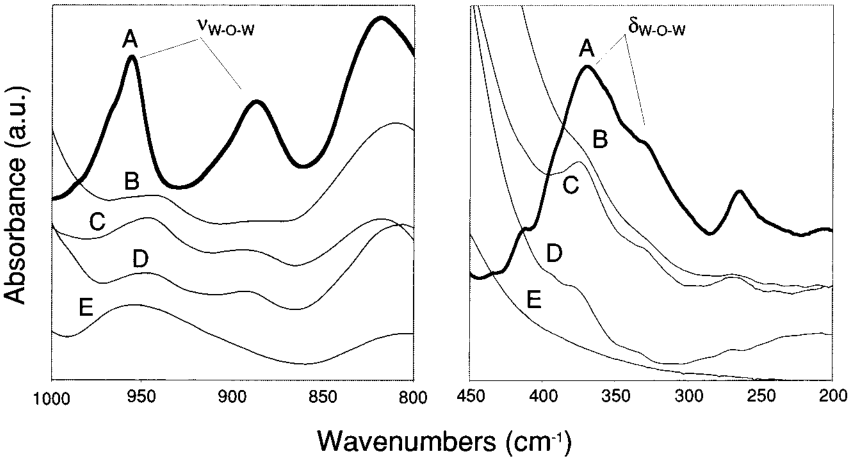

Figure 3. Midrange (left) and far-range (right) FT-IR spectra for (A) $K_5[CoPW_{11}]$; (B) macroporous silica/amine impregnated with $K_5[CoPW_{11}]$; (C) amorphous silica−amine impregnated with $K_5[CoPW_{11}]$; (D) amorphous silica−amine impregnated with $TBA_5[CoPW_{11}]$ after three catalytic cycles; (E) amorphous silica.

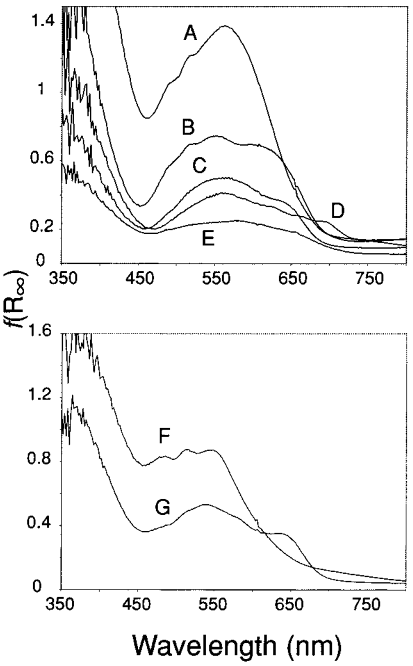

Figure 4. DR-UV−vis spectra of the TMSP materials. Top: (A) $K_5[CoPW_{11}]$; (B) amorphous silica−amine impregnated with $K_5[CoPW_{11}]$; (C) amorphous silica−amine impregnated with $TBA_5[CoPW_{11}]$; (D) amorphous silica−amine impregnated with $TBA_5[CoPW_{11}]$ after three catalytic runs; (E) macroporous silica−amine impregnated with $K_5[CoPW_{11}]$. Appearance of a shoulder in B, C, D, and E at 628−640 nm arises from coordination of the cluster to the surface amine, peaks in D at 660 and 692 nm are from Co^{III}. Bottom: (F) $K_9H[SiW_9Co_3]$; (G) amorphous silica−amine impregnated with $K_9H[SiW_9Co_3]$. The peak at 647 nm in G is due to coordination of the TMSP to the surface amine. Values of *f*(R∞) were calculated from the absorbance values using the Kubelka−Munk equation.

The ^{31}P MAS NMR of amine-functionalized silica impregnated with $TBA_5[ZnPW_{11}]$ (from acetonitrile solution) gave a single ^{31}P resonance at −12.4 ppm (Figure 6C), which was only slightly perturbed from the nongrafted cluster and indicated retention of the $[ZnPW_{11}]^{5-}$ structure. The perturbation of the P environment was attributed to interaction with the silica surface, which has been observed in previous studies involving various heteropoly anions on silica.[27,30,45−47] However, the ^{31}P solid state MAS NMR spectrum of $K_5[ZnPW_{11}]$ impregnated on amorphous silica/amine from an aqueous solution showed three distinct peaks at 0.5, −8.0, and −12.4 ppm (Figure 6B). The three P environments lead us to believe that the cluster underwent partial degradation in aqueous solution so that in addition to the major species ($[ZnPW_{11}]$, −12.4 ppm), the sample contained phosphate groups (0.5 ppm) and species such as cluster derivatives containing $[PW_9]$ units whose resonances typically fall in the range −8.0 to −14 ppm.[48]

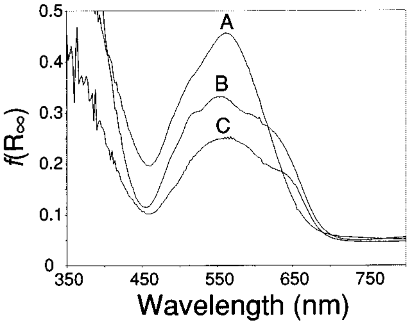

Figure 5. DR-UV−vis spectra of (A) amorphous silica + $K_5[CoPW_{11}]$, incipient wetness, λ_{max} = 560 nm; (B) amorphous silica/amine + $K_5[CoPW_{11}]$, λ = 628 nm; (C) amorphous silica/amine + $TBA_5[CoPW_{11}]$ (*x*, 2.5), λ = 638 nm.

These spectroscopic observations are consistent with information derived from elemental analyses of the TMSP−silica materials (Table 1). Samples prepared by stirring the amine-functionalized silica supports in nonaqueous solutions of $TBA_5[MPW_{11}]$ showed all the features expected for the amine-coordinated clusters in UV−vis, FT-IR, and ^{31}P NMR spectra, and M/P/W atomic ratios were reasonably close to those of the cluster precursor. We therefore conclude that in these samples the TMSP clusters were attached to the supports and most of them remained intact. Samples obtained by stirring the supports for 24 h in aqueous solutions of $K_5[MPW_{11}]$ salts also exhibited features of the original coordinated cluster in the UV−vis, FT-IR, and ^{31}P NMR spectra, but the ^{31}P NMR spectra displayed the additional resonances noted above. Elemental analyses of these latter samples revealed W/Co and P/Co ratios slightly lower than expected for intact clusters. It appeared that some

---

(45) Lefebvre, F. *J. Chem. Soc., Chem. Commun.* **1992**, 756.
(46) Chang, T. *J. Chem. Soc., Faraday Trans.* **1995**, *91*, 375.
(47) Mastikhin, V. M.; Kulikov, S. M.; Nosov, A. V.; Kozhevnikov, I. V.; Mudrakovsky, I. L.; Timofeeva, M. N. *J. Mol. Catal.* **1990**, *60*, 65.
(48) Massart, R.; Contant, R.; Fruchart, J.; Ciabrini, J.; Fournier, M. *Inorg. Chem.* **1977**, *16*, 2916.

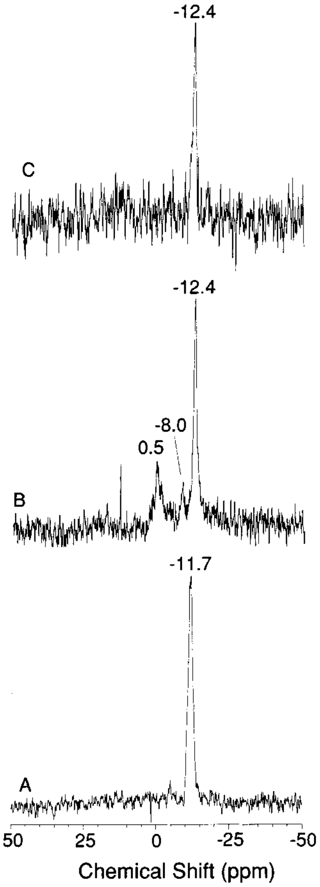

Figure 6. Solid-state ^{31}P MAS NMR of (A) TBA$_5$[ZnPW$_{11}$]; (B) amorphous silica−amine + K$_5$[ZnPW$_{11}$]; (C) amorphous silica−amine + TBA$_5$[ZnPW$_{11}$].

W and P was lost from the sample, implying partial cluster degradation. In the zinc-substituted clusters the decomposition products were still observed by ^{31}P NMR. In the other samples decomposition products not containing Co may have been washed off, much as in experiments with [PW$_{11}$] clusters (Table 1, sample D), while the free Co was retained by the amine ligands. Partial cluster degradation could be caused by an increase in pH due to the surface amines. Final pH values were calculated to be between pH 7.6 and 7.9, based on the amounts of amine groups present in the volume of water used. At these pH values, some degradation of the TMSP was possible, as the monosubstituted TMSP clusters are stable up to pH 7. However, even in the samples prepared from aqueous solution, the combined spectroscopic evidence showed that the majority of the attached clusters remained intact. After characterization of the binding and structure of the TMSP on the silica surface, the materials were tested for their catalytic activity.

Catalytic Testing. The catalytic activities of supported and unsupported cobalt-substituted POM clusters were tested by studying the conversion of cyclohexene to cyclohexene oxide in the presence of isobutyraldehyde. Results from these reactions, percent conversion, and moles of cyclohexene oxide produced per second after a 1 h reaction time are listed in Table 4. Proton-decoupled ^{13}C NMR spectra were used to identify the products, which were quantified based on the integrated areas of the corresponding ^{1}H NMR spectra. No other products of cyclohexene oxidation were detected, although other byproducts arose from the oxidation of isobutyraldehyde, as determined by performing the reaction without cyclohexene. The absence of other cyclohexene oxidation products indicated that the selectivity for cyclohexene oxide production approached 100%.

Table 4. Comparison of the Catalytic Activity of [CoPW$_{11}$]$^{5-}$ and [SiW$_9$Co$_3$]$^{10-}$ TMSP−Silica Materials for the Oxidation of Cyclohexene to Cyclohexene Oxide[a]

catalyst	mol cyclohexene oxide produced/s (mol/s, $\times 10^{-8}$)	conversion of cyclohexene (1 h) (%)
no catalyst	0.4 ± 0.1	2.0 ± 0.5
solid K$_5$[CoPW$_{11}$]	0.6 ± 0.2	7.0 ± 1.0
homogeneous [CoPW$_{11}$]$^{5-}$ [b]	13.8 ± 0.5	76.5 ± 6.4
amorphous silica + amine + TBA$_5$[CoPW$_{11}$]	6.9 ± 2.8	45.2 ± 1.4
amorphous silica + amine + K$_5$[CoPW$_{11}$]	9.5 ± 1.2	46.5 ± 5.3
macroporous silica + amine + K$_5$[CoPW$_{11}$]	10.1 ± 2.2	61.9 ± 17.5
MCM-41 + amine + K$_5$[CoPW$_{11}$]	7.8 ± 1.8	57.3 ± 12.9
homogeneous [SiW$_9$Co$_3$]$^{10-}$ [b]	19.3 ± 1.9	92.8 ± 4.5
amorphous silica + amine + K$_{10}$[SiW$_9$Co$_3$]	16.4 ± 3.0	90.9 ± 4.7

[a] Reaction conditions: 0.75 μmol TMSP, 750 μmol cyclohexene, 3000 μmol isobutyraldehyde, 224.2 μmol benzene (int std), 7 mL CDCl$_3$. Values were averaged from a minimum of three runs for each sample. One standard deviation is given. [b] TBA salts of these clusters were dissolved in CDCl$_3$ by adding stoichiometric amounts of [CH$_3$N$^+$(CH$_2$)$_7$CH$_3$)$_3$] as counterion.

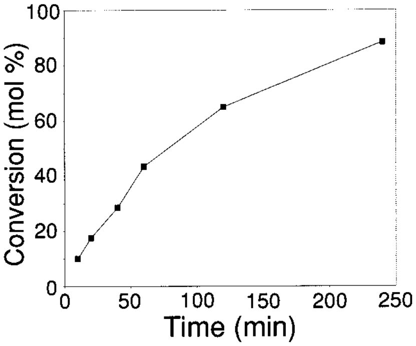

Figure 7. Time course of catalytic test reaction. Catalyst: amorphous silica + amine + TBA$_5$[CoPW$_{11}$]. Conversion is recorded as mol % cyclohexene consumed.

A graph depicting the time course of cyclohexene conversion for amorphous silica/amine impregnated with TBA$_5$[CoPW$_{11}$] is provided in Figure 7. The reaction carried out with trisubstituted [SiW$_9$Co$_3$] clusters gave almost complete conversion of cyclohexene to cyclohexene oxide within 1 h with no observable byproducts of cyclohexene oxidation.

The reactivity of the supported [CoPW$_{11}$] clusters was lower than that of the clusters in homogeneous reactions. Their activity was similar on all three supports within experimental error. [SiW$_9$Co$_3$] clusters exhibited significantly higher production of cyclohexene oxide per second than the monosubstituted species in homogeneous solution and especially when supported. The greater catalytic activity was most likely due to the higher number of Co^{II} centers available for reaction.

To understand these results, the reaction mechanism is summarized here briefly according to the literature.[12,13,49] The reaction between the aldehyde and the transition metal site of the TMSP produces acyl radicals, which in turn react with dioxygen to produce acyl peroxy radicals. The acyl peroxy radicals have several pathways by which to react, but the most relevant to this study is the reaction with aldehydes present in solution to form acyl peroxy acids. The acyl peroxy acids are

---

(49) Nam, W.; Kim, H. J.; Kim, S. H.; Ho, R. Y. N.; Valentine, J. S. *Inorg. Chem.* **1996**, *35*, 1045.

Scheme 2

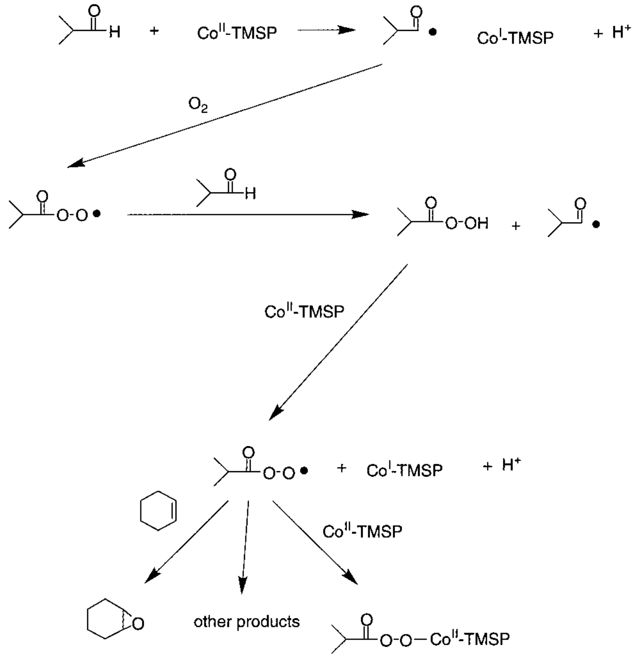

decomposed efficiently by the Co^{II}-TMSP to acyl peroxy radicals, which are the true epoxidizing agents. Since the Co^{II} site is effective at decomposing acyl peroxy acids, the majority of acyl peroxy radicals are produced in this way, rather than by the reaction of acyl radicals with oxygen.[12] The Co^{II} centers may also react with the acyl peroxy radicals to form metal−peroxy species, which effectively inhibits the production of epoxide. Other side reactions produce the carboxylic acid, CO_2 and ketones.[12,13] A simplified reaction mechanism focusing on the species of interest for this discussion is provided in Scheme 2.

When the reaction mechanism described above is considered, the reduced performance of supported TMSPs can be attributed to interactions of the catalytically active site with the support. Diffusion limitations of the aldehyde and acyl peroxy acids to the Co^{II} centers and of the acyl peroxy radicals away from the solid surface may reduce the catalytic performance. Another factor in the catalytic reactivity should be the surface area of the support. It was found that the amorphous and macroporous silicas had similar surface areas, and therefore, no surface area effects were evident. Samples supported on MCM-41 were expected to have greater loading and dispersion of TMSP clusters, but since the pore volume was not fully accessible, the number of catalytic sites, and therefore the reactivity, was similar to the other silica supports. The test reaction studied here involves the TMSP only for the production of the epoxidizing agent (acyl peroxy radicals). It is not necessary for the cyclohexene to react directly with the TMSP. Because of this fact, the actual structure of the support does not directly affect the production of epoxide. The support does, however, play an important role in the ease of separation, and the effects of dispersing the TMSP clusters are evident when comparing the results obtained with solid $K_5[CoPW_{11}]$ and the analogous supported and dispersed TMSPs on any of the silica supports.

Catalyst materials were cycled through multiple catalytic runs without loss of activity. DR-UV−vis and far-FT-IR spectra were performed on a sample of amorphous silica/amine + $TBA_5[CoPW_{11}]$ that had been used in three catalytic cycles (see Figure 3D and Figure 4D). DR-UV−vis showed the retention of the charge-transfer band and coordinated octahedral Co^{II}. New visible absorbances at 660 and 692 nm are observed, which are evidence for the presence of a small amount of Co^{III}. Mid- and far-FT-IR spectra exhibited ν_{W-O-W} bands at 890 cm^{-1} and δ_{W-O-W} bands at 370 and 332 cm^{-1}, respectively, in agreement with spectra obtained on precatalysis samples. This leads us to believe that, during catalysis, the TMSP remains intact with the only changes involving redox reactions of the Co site.

Elemental analysis of the catalysts before and after reaction showed that, for the $[CoPW_{11}]$−silica materials, 98.3 wt % of TMSP remained on the support (i.e., 0.08 μmol was lost into solution during the reaction), while for the $[SiW_9Co_3]$−silica materials, all TMSP remained on the support. The slight loss of the monocobalt-substituted cluster may be due to competition between acyl peroxy radicals and surface ligands for the single transition metal center of the cluster. It was also possible that during the course of the reaction, the monosubstituted TMSP detached from the surface, reacted homogeneously, then either reattached to the surface ligand or bound an acyl peroxy radical, and was lost into solution. Trisubstituted TMSP clusters have two accessible Co^{II} centers in addition to the amine-bound cobalt site. These can bind acyl peroxy species at the completion of the reaction cycle without affecting the surface attachment. This resulted in a greater retention ability on the surface.

Conclusion

The procedure presented in this paper, using Co- and Zn-substituted POM clusters as examples, is a general method for anchoring TMSP clusters to the surface of silica supports. Evidence for attachment of TMSP clusters to the silica surface was provided by several spectroscopic techniques. FT-IR spectra showed characteristic stretching and bending modes of the TMSP clusters. ^{31}P MAS NMR of the silica-supported $[ZnPW_{11}]$ clusters confirmed retention of the cluster structure when the clusters were added from acetonitrile solution, but provided evidence for partial degradation of $K_5[ZnPW_{11}]$ from aqueous impregnation. DR-UV−vis spectroscopy indicated that the TMSP was coordinated to the surface ligand, resulting in the observed splitting of the $^4T_{1g}$ band of the Co^{II} absorbance. On the other hand, when the TMSP was impregnated by incipient wetness onto unmodified silica, no splitting of the absorption occurred due to a lack of significant interaction with the support and the clusters were easily removed by washing. The supported $[CoPW_{11}]$ clusters were catalytically active, but slightly less so than their analogues in homogeneous solution. $[SiW_9Co_3]$ clusters with three available cobalt centers exhibited higher catalytic activity with nearly identical performance on a silica support or in homogeneous solution.

The major advantage of the supported TMSP clusters over homogeneous TMSPs was not their reactivity but the ease in separation and recovery of the solids containing highly dispersed clusters. The materials could be recycled through multiple reactions without loss of activity and were recovered by filtration. In the case of monosubstituted $[CoPW_{11}]$ clusters, a small fraction of the clusters leached into solution during the reaction but all trisubstituted $[SiW_9Co_3]$ clusters were retained during the catalytic reaction.

Acknowledgment. The authors thank the National Science Foundation (DMR-9701507 and the MRSEC program of the NSF under Award Number DMR-9809364), 3M, Dupont, and the David and Lucile Packard Foundation for funding. We also thank Rick Knurr, Department of Geology, University of Minnesota, for elemental analyses.

IC991440Y